Refitting of an eco-friendly sailing yacht: numerical prediction and experimental validation

A. MANCUSO[1], G. PITARRESI[1], G.B. TRINCA[1] and D. TUMINO[2*]

[1] Università degli Studi di Palermo, DICGIM, Viale delle Scienze, Palermo 90128, Italy

[2] Università degli Studi di Enna Kore, Facoltà di Ingegneria e Architettura, Cittadella Universitaria, Enna 94100, Italy

* Corresponding author. Tel.: +39-935-536-491; E-mail address: davide.tumino@unikore.it

Abstract A 4.60 m sailing yacht, made with a flax fiber composite and wood, has been refitted with the aim of hull weight reduction and performance improvement during regattas. The first objective was obtained with a lightening of internal hull reinforcements while the second one with a reduction of the maximum beam, in order to minimize the longitudinal moment of inertia. The refitting was first simulated via CAD-FEM interaction to establish the feasibility of the procedure and to verify the structural integrity. The resulting hull was then instrumented with strain gauges and tested under typical rigging and sailing conditions. Results obtained by the numerical modeling and measured from experiments were compared.

Keywords: Parametric design, Refitting, Sailing yacht.

1 Introduction

The design of high performance racing yacht is a very complex activity. The goal is the better compromise between lightness and stiffness. This objective can be achieved only if a structured design approach is followed [1]. In this perspective, an accurate estimation of internal loads (rigging) and external loads (aero/hydro) becomes fundamental. Internal loads can be easily obtained from equilibrium static conditions, once the type of rigging is established (with or without spreaders, fractional, etc.). An accurate prediction of aero/hydro dynamic forces is instead more complex, usually requiring time consuming numerical CFD simulations [2]. Some works approaching the problem with numerical modelling comprise [3,4], where the authors take into account the slamming effect which leads to relevant loads, and [5] where the uncertainty of several variables (composite fibre orientation, mechanical properties, etc.) is also considered. Some exper-

B. Eynard et al. (eds.), *Advances on Mechanics, Design Engineering and Manufacturing*, Lecture Notes in Mechanical Engineering,
DOI 10.1007/978-3-319-45781-9_53

imental approaches have also been attempted, such as in [6] where the structural integrity of a IACC yacht is monitored via fiber-optic sensors. The studied yachts are generally short-life designed, so that long term effects on structural performances are usually neglected in the design approach. Although several papers are found in literature concerning the design of mid-large racing yachts, to the authors knowledge, much little information is available regarding small boats as dinghies. The present study has focused on the re-engineering of a 15' SKIFF type sailing yacht. The numerical Finite Element Method (FEM) is proposed to model the hull and deck, made of plywood and a *green sandwich* composite with a Flax Reinforced Epoxy skin laminate. The paper focuses on the analysis performed to model a system of simplified loads, based on rigging and navigation conditions. The model is then validated by means of Electrical Resistance strain gauges installed in different locations of the hull and frame structure, which provide a local measure of the deformation state that is compared with the FEM prediction.

2 Methods

A simultaneous engineering design approach, similar to [7-9], has been applied based on full integration between numerical simulations and experimental data. The analyzed dinghy has been refitted with the aim of a weight reduction, obtained by cutting and removing parts of the internal frame and hull. The refitting was in particular designed to achieve performance improvements during regattas, by reducing the maximum beam, in order to minimize the longitudinal moment of inertia. The final shape obtained after an accurate FEM investigation, is shown in fig. 1. The weight reduction with respect to the original shape was of about 19% (from 88 kg to 71 kg.).

Electrical Resistance strain gauges (ER) have been applied in order to obtain local measurements of strain components to be compared with the corresponding numerical predictions. In particular, four three-grid rectangular rosettes (HBM type RY81-6/350) and four single grid (HBM type LY11-6/350) ER gauges have been installed on specific locations chosen from preliminary FEM analyses. These locations are shown in Fig. 1: the rosettes are bonded on the upper lamina (inboard side) of the sandwich hull material, while single grids are bonded on the plywood frame structure. A three letters nomenclature is proposed, where the first letter (S, R) stands for Single grid or Rosette; the second letter (K, W, A, S) stands for Keel, Web frame, Ahead, Stern, respectively. The last letter (S, P) stands for Starboard side and Port side. ERs SKS, SWS, RAS, RSS are approximately symmetric about the central beam keel to respectively SKP, SWP, RAP, RSP.

Care was taken in order to orient the grids of rosettes with the same angles with respect to the local fibers direction. It is though noticed that misalignment errors [10] would not affect the values of calculated principal strains, so the comparison with numerical predictions in Section 3.3 is performed on the maximum principal

strains. All grids have been wired up with four wires and protected with a polyurethane paint HBM type PU120 and a silicone sealing layer HBM type SG250.

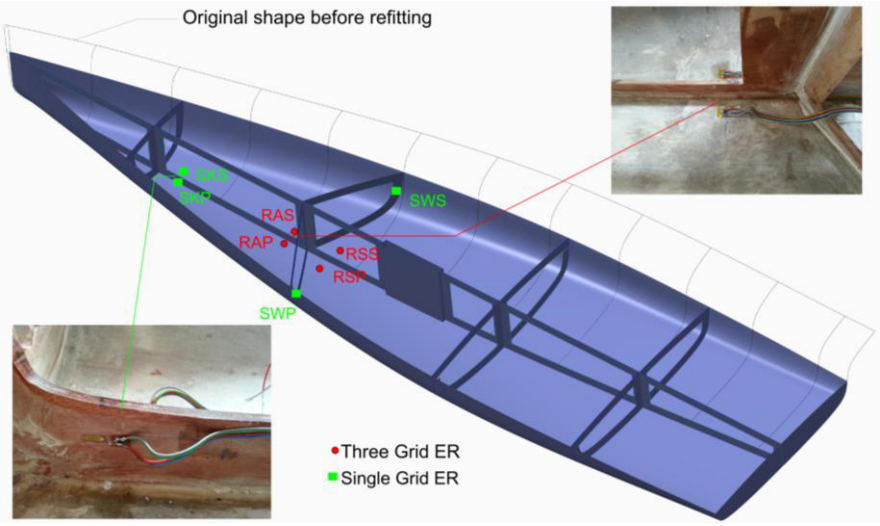

Fig. 1. CAD model of the dinghy after refitting, and location of strain gauges with nomenclature.

One rosette and one single grid ER were also prepared for use as dummy gauges for temperature compensation on equivalent pieces of sandwich and plywood.

For the evaluation of the rigging loading in the lab, a multichannel HBM UPM100 data logger was used to connect all ERs and synchronously acquire all signals at a sampling rate of about 1 Hz. Each grid was connected using a quarter bridge 4 wire scheme. The dummy gauges were connected and monitored as separate quarter bridge channels. All active and dummy gauges have been preliminary monitored for 20 minutes with the boat under unloaded conditions, and all ERs showed no significant thermal drift, with the signals oscillating between ±1 μm/m.

3 Numerical simulations

Numerical simulations have been performed starting from the complete CAD model prepared in CREO Parametric (from PTC). The software package ANSYS R.15 was used to setup different aspects of the simulation. Some practical assumptions have been adopted to determine the loading conditions: analytical equilibrium equations are used together with numerical simulations in the Mechanical APDL environment. The complex bio-sandwich material used for the hull [11, 12] is modelled by means of the ACP PrePost. Structural analyses are performed in Workbench where different load cases are simulated.

3.1 Estimation of loads

The main procedural assumption made for the simulations is to replace the rig with an equivalent system of forces exerted by the rig on the boat, i.e. at the connections of forestay and shrouds with the deck and at the mast foot. Determination of the loads on the rig considers two different conditions: the preload (rigging) applied on the system and the combination of aerodynamic forces from the main sail and weight of the crew.

Preload on mast, shrouds and forestay can be calculated by solving the equilibrium equations in the cartesian reference frame; this is a self-balanced system of forces necessary to compensate the load variations on the rig during navigation. After preload, the mast is subject to a pure compressive load, while shrouds and forestay to pure tension loads. Two values of preload on the mast has been established, and the resulting rigging loads are then calculated and reported in Table 1. The smaller preload (Rigging 1) is applied on the boat when the deck was not yet joined to the hull. The higher preload (Rigging 2) was applied when the boat was complete with the connection of the deck. The sign of values reported in Table 1 refers to the prevalent action of the load: negative is for loads pushing the deck downward and positive for loads pulling the deck upward. The rigging forces are readily applied in the model at the connection points between the rig and the deck.

The second load system is the one that comes from the equilibrium between aerodynamic, fluid dynamic and weight forces [13]. Figure 2 shows forces used for the equilibrium in planes *yz* and *xz*. In figure 2 (left) the equilibrium of the moments around the *x* axis is considered with respect to the centerboard, while in figure 2 (middle) the equilibrium of moments around the *y* axis is considered with respect to the center of buoyancy.

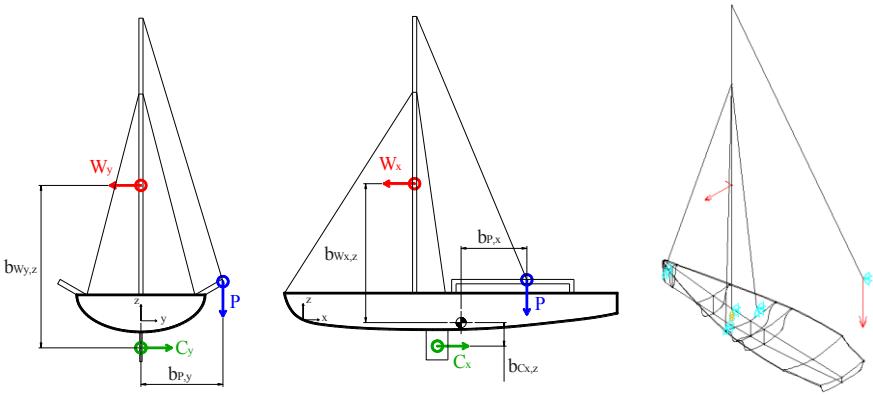

Fig. 2. Equilibrium of moments around *x* (left) and around *y* (middle). Model in APDL used to calculate loads on the deck due to wind and crew weight actions (right).

Resulting equations are as follows:

$$P \cdot b_{Py} = W_y \cdot b_{Wy,z} \tag{1}$$

$$P \cdot b_{Px} = W_x \cdot b_{Wx,z} \tag{2}$$

where, for eq. (2), the moment due to the hydrodynamic force on the hull and on the centerboard has been neglected due to the small distance between the resulting axis and the center of buoyancy. The weight of the crew is assumed P = 1500 N, while distances $b_{P,x}$ and $b_{P,y}$ are geometrically determined. Distance $b_{Wy,z}$ (or similarly $b_{Wx,z}$) comes from the evaluation of the center of pressure on the main sail, see [13] for details. Components of the aerodynamic force W are then calculated as W_x = 230 N and W_y = 960 N.

The aerodynamic force is applied to the center of pressure on the main sail, and is equilibrated by the crew and the hydrodynamics of the hull and centerboard. The aerodynamic force and the crew weight can be transferred to the rig by analytically solving the equilibrium equations or by modeling the rig with FEM. In this study the Mechanical APDL module is used to model the rig with beam and link as shown in figure 2 (right). Reactions calculated in this analysis (Table 1, last row) can then be applied to the connection points of the rig to the deck, and the resultant forces are obtained by algebraically adding the navigation forces to the preloads.

The weight of the boat is 900 N and is considered as a volume distributed load and, added to the crew weight, equals the displacement of the hull, ∇ = 2400 N. It is assumed that the boat runs flat during navigation, hence no pitch and roll angles are considered. No hydrodynamic effect is considered on the hull; an hydrostatic pressure distribution is applied to the hull in order to equilibrate the total weight of boat and crew regardless to any modification of the floating line caused by the speed of navigation. In section 3.4 an extreme case will also be simulated where the boat is supported on two waves at stern and bow, corresponding to the physical condition of incipient pre-planning navigation.

Finally, another force to be considered on the boat is given by the hydrodynamic actions on the centerboard. In this paper, instead of using numerical techniques as inertia relief [14, 15], we evaluate this force as reaction, applied on the trunk of the centerboard, able to equilibrate the above mentioned external loads and keeping a flat trim on the sea.

Table 1. Loads [N] on rig.

Configuration	*Mast*	*Upwind shroud*	*Downwind shroud*	*Forestay*
Rigging 1 (with deck)	-3000	1323	1323	387
Rigging 2 (without deck)	-3630	1600	1600	469
Navigation	-1991	-809	32	1235

3.2 FEM model

Once internal and external loads are determined, the CAD model of the boat is implemented in the Workbench environment. Due to the complexity of the elastic behavior of the composite sandwich used for the hull, the material has been defined using the ACP PrePost. A mechanical characterization of the flax composite skin and cork core has been performed in previous works [11, 12]. The elastic constants of the unidirectional ply and the stacking sequence of the plies are defined in the ACP in order to obtain an oriented layered section of the hull material. The sequence used is [0/45/-45/90/cork/90/-45/45/0]. Direction 0° is aligned with the longitudinal x axis. All other components of the boat, i.e. web frames, keel, trunk and deck, are made of marine plywood.

The element type used for the FE model is the four-noded SHELL181, with membrane plus flexural behavior. In the case of components made of marine plywood the element has a specified thickness, while, for the sandwich hull, is associated to a layered section. All connections between components are assumed to be perfectly bonded. The resulting mesh is constituted by 120172 regular quadrilateral elements. Average dimension of the element side is approximatively 10 mm, but in some specific areas, where resistance gauges are located, mesh refinements are defined. The orthotropy of the material defined in the ACP module is associated to a linear elastic constitutive model implemented in the APDL solver.

According to considerations done in 3.1, displacements are constrained along x at stern to equilibrate W_x, and along y at the trunk level to equilibrate the heeling moment given by W_y and P.

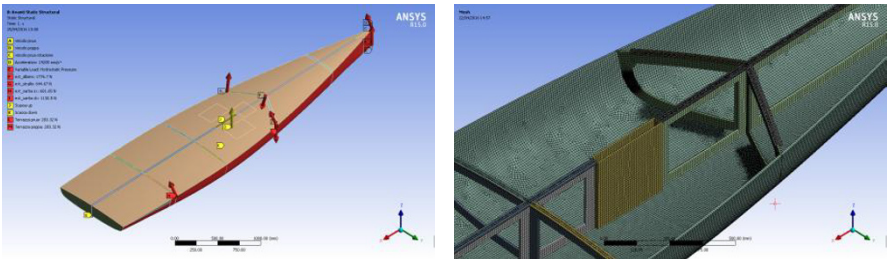

Fig. 3. (left) loads applied to the FEM model; (right) FEM model of the boat and particular of the mesh.

3.3 Validation with experiments

Experimental data for the validation of the FEM model are provided by measuring the strains from ERs (see Section 2.2), under the action of rigging loads. The

boat has been rigged in two different configurations (with and without the deck), and at different preload levels. Rigging loads up to 1600 N (measured on the shrouds by a load cell and reported in Table 1) were applied, and ER data were observed to grow linearly within this range of loads.

User coordinate systems are created in correspondence to the location of single grid ER and rosettes (see fig. 3). The deformation values predicted by the FEM model are calculated along the directions corresponding to the ERs orientations. The three deformations corresponding to the three grids of rosettes were in particular taken from the deformations of the upper in-board lamina of the hull sandwich. These deformations were further combined to derive principal strains to be compared with the equivalent experimental value. The particular self-equilibrated set of rigging loads influences mainly the portion of the boat between shrouds and forestay, leaving the aft portion substantially unloaded, see fig. 3 (right).

Table 2 reports experimental and numerical strains for the two configurations with and without deck. A good agreement can be generally noted, especially for the single grid ERs. It must be remarked that all ERs are placed in high gradient strain areas and small errors in the localization of the measuring point can easily result in significant departures between experimental and numerical results. In the worst case, the maximum difference does not exceed 18% and, because of uncertainties due to the localization of ERs, symmetry of structures, fiber alignment, etc. these level of error is considered satisfactory.

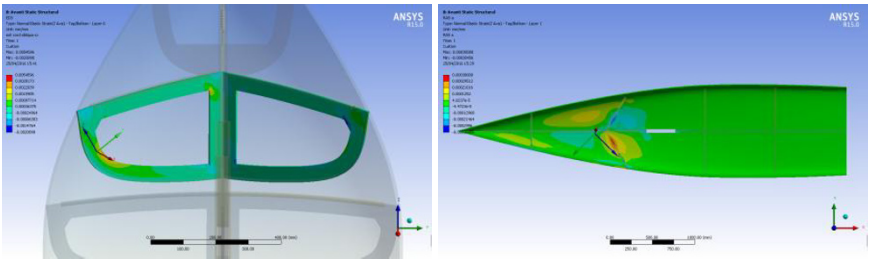

Fig. 3. Maps used to calculate the strain in correspondence of SWP (left) and of RAP (right). Local triads are positioned and aligned as ERs.

Table 2. Strains [μm/m] obtained with experiments and FEM.

Configuration	*Method*	*SKS*	*SKP*	*SWS*	*SWP*	*RAS*	*RAP*	*RSS*	*RSP*
Rigging 1	Experiments	508	434	2474	2100	319	276	245	194
	FEM	465	396	2190	1997	327	325	245	228
	error %	8.5	8.8	11.5	4.9	-2.6	-17.8	-0.3	-17.5
Rigging 2	Experiments	311	256	1276	1144	-	-	-	-
	FEM	310	270	1310	1220	-	-	-	-
	error %	0.3	-5.5	-2.7	-6.6	-	-	-	-

3.4 Load cases

Section 3.3 has demonstrated the reliability of the FEM model to reproduce deformations of the boat when subject to simple rigging preload. It is now interesting to simulate real navigation conditions that are difficult to reproduce in laboratory, and require measurements to be performed during tests at sea. At this purpose, four operative conditions are simulated for the boat (see also Fig. 4):

- C1: only rigging with a load on shrouds of 1600 N,
- C2: floating on flat sea with loads due to rigging, hydrostatic pressure and the crew sit on center of the deck,
- C3: navigation on flat sea with loads due to rigging, aerodynamic and hydrostatic pressure and the crew on trapeze,
- C4: navigation on rough sea with loads due to rigging, aerodynamic pressure and the crew on trapeze.

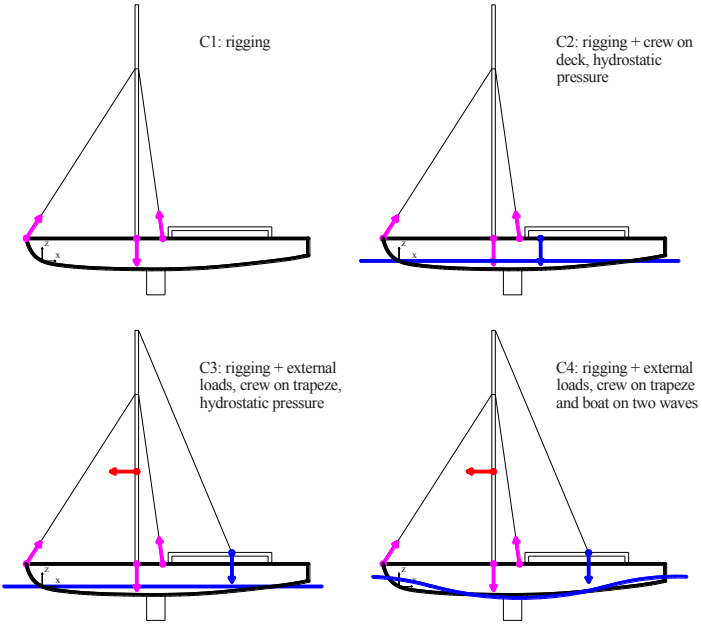

Fig. 4. Load configurations used in FEM simulations.

Results of FEM simulations are summarized in Fig. 5. These are presented in terms of the strains that would be measured by the installed ERs. In the configuration C4 the boat is supposed to be constrained only at bow and stern (i.e. standing on two waves peaks) and no uniform hydrostatic pressure is applied on the hull. Some considerations arise as follows.

Strains on the keel (SKS and SKP) are symmetric in all conditions. Instead, strains on SWS and SWP differ significantly when navigation conditions are ap-

plied. The SWS strain in the downwind side is more than twice the SWP strain in the upwind. It is then a general rule for this kind of boat that the downwind shroud overloads the point of connection to the deck in order to equilibrate the weight of the crew on trapeze. Configurations C1 and C2 are very similar. Configuration C4 generally increases the strain level with respect to C3, especially on the keel.

Regarding the hull strains (represented by the maximum principal strain at the rosettes locations), a symmetric behavior is obtained for the areas ahead of the mast (RAS and RAP). In the locations behind the mast of RSS and RSP strains are more sensitive to navigation loading conditions. In particular, the downwind side (RAP) has a higher increase of strain than the upwind side (RAS). In general, hull maximum strains under C4 reach higher levels compared to C3, in particular for the locations ahead of the mast.

In general, it is noted that during navigation the level of strains on the framing plywood structure and on the hull can double the one due only to rigging.

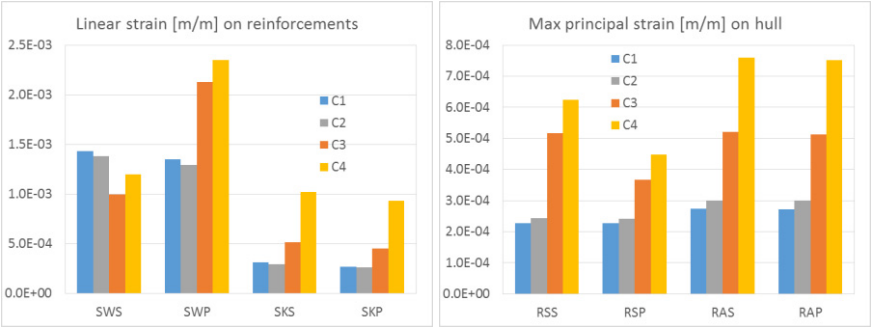

Fig. 5. Calculation of strains form simulations for different operative conditions.

4 Conclusions

The present work has described a FEM model of a complete sailing dinghy. The structure is composed by a hull made of a sandwich with cork core and flax reinforced epoxy skins, a deck and an internal framing rig of plywood. The numerical model implements materials constitutive behaviors developed from previous experimental mechanical characterizations. In order to verify the model, electrical resistance single and three grid rosette strain gauges have been installed at specific locations of the hull and framing structures. Experimental strains have been measured under a symmetric rigging loading, and compared with equivalent strains from the FEM model. This comparison provided fairly small differences (below 18%), reckoned acceptable for the level of complexity of the analyzed structure, thus providing good confidence in the prediction capabilities of the developed FEM model.

Some different loading configurations have also been simulated and studied numerically, representing complex scenarios as navigation under flat or rough sea. The values of strains obtained with FEM on various boat locations are consistent with the expected boat behavior. Future work will attempt to use the installed strain gauges to measure strains during real navigation conditions, in order to provide further confirmation of the effectiveness of the FEM model also in complex navigation conditions.

Acknowledgments The authors are grateful to ANSYS and HBM for their support given on scientific activities of the project. A particular thank also goes to the Zyz Sailing Team students that participate to manufacturing and racing activities.

References

1. Ingrassia T., Mancuso A., Nigrelli V., Tumino D. A multi-technique simultaneous approach for the design of a sailing yacht. International Journal on Interactive Design and Manufacturing, Article in Press. DOI: 10.1007/s12008-015-0267-2.
2. Alaimo A., Esposito A., Messineo A., Orlando C., Tumino D. 3D CFD analysis of a vertical axis wind turbine. Energies, 2015, 8(4), 3013-3033.
3. Allen T., Battley M., Casari P., Kerling B., Stenius I., Westlund J. Structural Responses of high Performance Sailing Yachts to Slamming Loads. 11th International Conference on Fast Sea Transportation FAST, 2011, Honolulu, Hawaii, USA.
4. D. Kelly, C. Reidsema, A. Bassandeh, G. Pearce, M. Lee. On interpreting load paths and identifying a load bearing topology from finite element analysis. Finite Elements in Analysis and Design, 2011, 47, 867–876.
5. Lee M.C.W., Payne R.M., Kelly D.W., Thomson R.S. Determination of robustness for a stiffened composite structure using stochastic analysis. Composite Structures, 2008, 86, 78–84.
6. Murayama H., Wada D., Igawa H. Structural Health Monitoring by Using Fiber-Optic Distributed Strain Sensors With High Spatial Resolution. Photonic Sensors, 2013, 3(4), 355–376.
7. Cerniglia D., Ingrassia T., D'Acquisto L., Saporito M., Tumino D. Contact between the components of a knee prosthesis: Numerical and experimental study. Frattura ed Integrità Strutturale, 2012, 22, 56-68.
8. Ingrassia T., Nigrelli V., Buttitta R. A comparison of simplex and simulated annealing for optimization of a new rear underrun protective device. Engineering with Computers, 2013, 29, 345-358.
9. Ingrassia, T., Nigrelli, V., Design optimization and analysis of a new rear underrun protective device for truck. Proceedings of the 8th International Symposium on Tools and Methods of Competitive Engineering, TMCE 2010, 2, 713-725.
10. Ajovalasit A., Cipolla N., Mancuso A. Strain Measurement on Composites: Errors due to Rosette Misalignment. Strain, 2002, 38, 150-156.
11. Mancuso A., Pitarresi G., Tumino, D. Mechanical Behaviour of a Green Sandwich Made of Flax Reinforced Polymer Facings and Cork Core. Procedia Engineering, 2015, 109, 144-153.
12. Pitarresi G., Tumino D., Mancuso A. Thermo-mechanical behaviour of flax-fibre reinforced epoxy laminates for industrial applications. Materials, 2015, 8(11), 7371-7388.
13. Larsson L., Eliasson R.E. Principles of yacht design, 1996 (Adlard Coles Nautical, London).
14. Alaimo A., Milazzo A., Tumino, D. Modal and structural fem analysis of a 50 ft. pleasure yacht. Applied Mechanics and Materials, 2012, 215-216, 692-697.
15. Bamett A.R., Widrick T.W. Ludwiczak D.R. Closed-Form Static Analysis With Inertia Relief and Displacement-Dependent Loads Using a MSC/NASTRAN DMAP Alter. NASA TM 106836, 1995.